

# Monitoring and Numerical Modelling of Induced and Triggered Seismicity in a Deep Sublevel-Stoping Mine

Francesca De Santis <sup>(1,2)</sup>, Yann Gunzburger <sup>(2)</sup>, Vincent Renaud <sup>(1)</sup>

Isabelle Contrucci<sup>(1)</sup>, Pascal Bernard<sup>(3)</sup>

(1) Institut National de l'Environnement Industriel et des Risques (Ineris); (2) GeoRessources, Université de Lorraine; (3) IPGP



# Objective of the study

## *Why compare seismic and model data?*

### *Microseismic Monitoring*

Real-time monitoring for short-term prevention

Advantages	Limits
Global in site measurements	Precision of detection and location
Real time monitoring	No detection of aseismic deformation
Insight into fractures dynamic	Local measures

### *Numerical modelling*

Optimization of future excavations

Advantages	Limits
Long-term prediction	Needs lots of geo-mechanical information
Simulation of different excavation sequences	High computational requirements
Global view of stress changes	

## *Finding possible links*

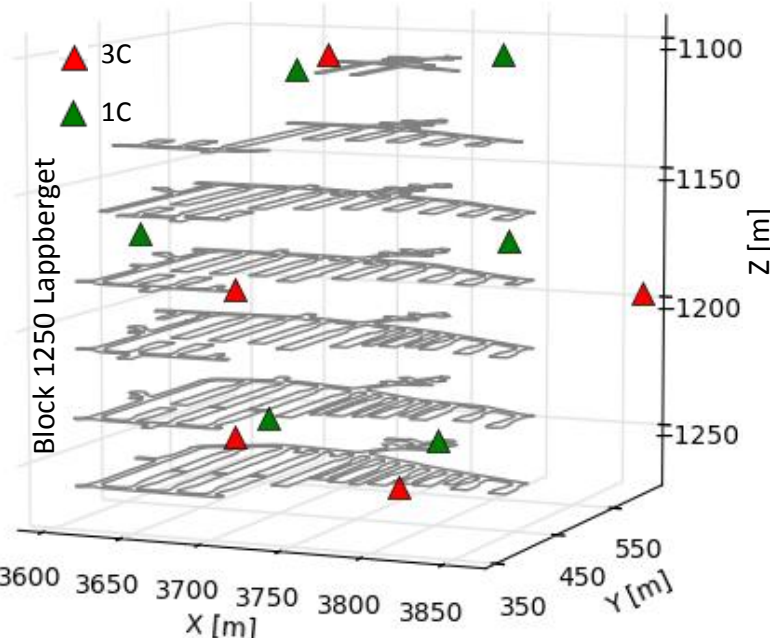
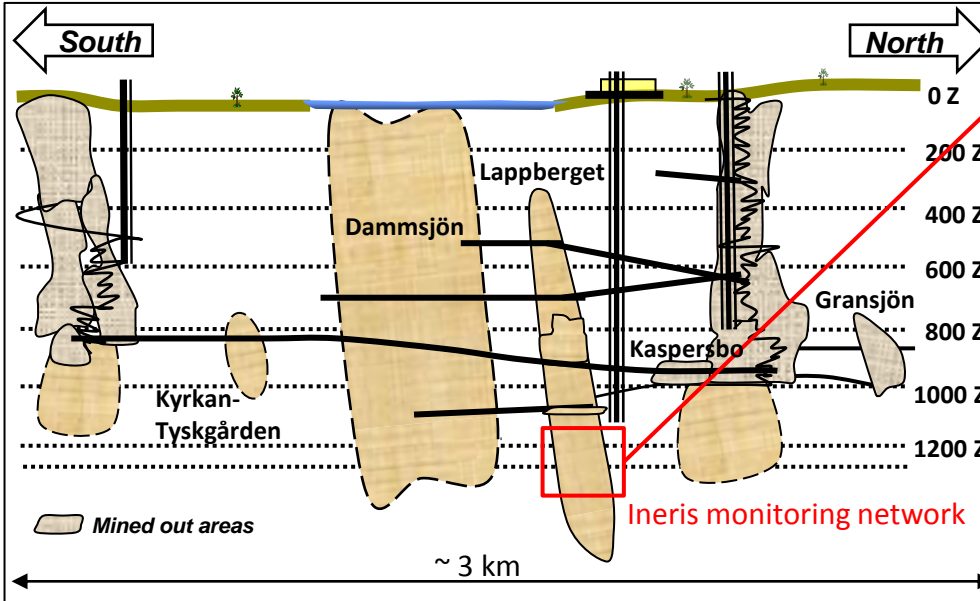
- Better understanding of interactions between stress changes and seismic activity generation
- Gaining additional insights into failure processes
- Improving long-term and short-term prevention

# Garpenberg mine

## Geographic and Historical context



Schematic vertical profile of Garpenberg mine

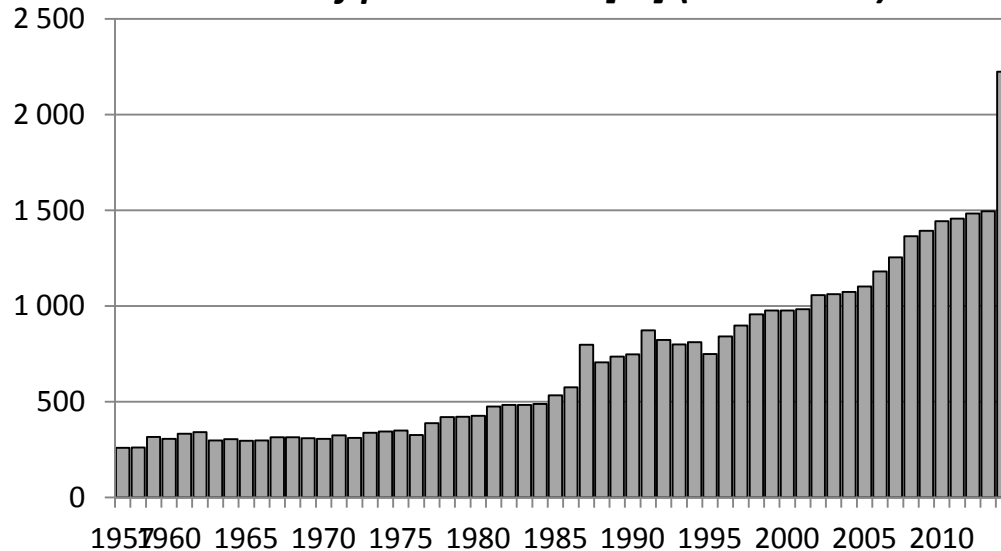


- Sv
- D $\epsilon$
- Acquired by Boliden in 1957 (300.000 tonnes/year)
- Discovery of Lappberget orebody in 1998
- Production moved in Garpenberg North in 2004

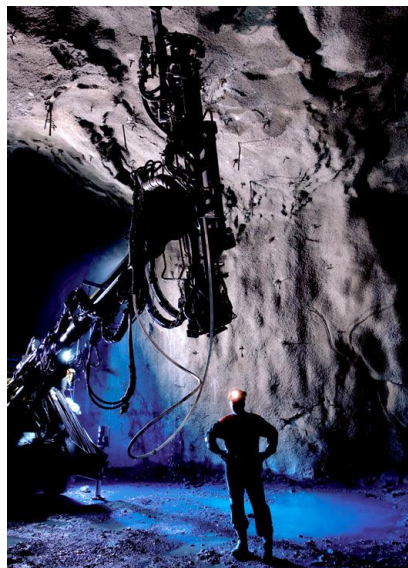
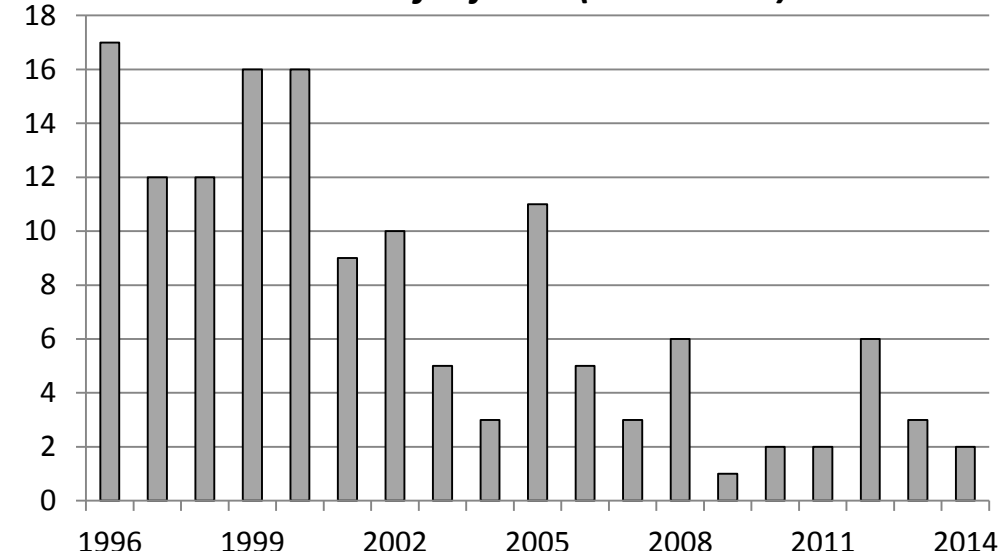
# Garpenberg mine

## Production & Injuries

*Amount of produced ore [kt] (1957-2014)*



*Number of injuries (1996-2014)*



*Mass mining methods*



*Improve automation  
and digitalization*

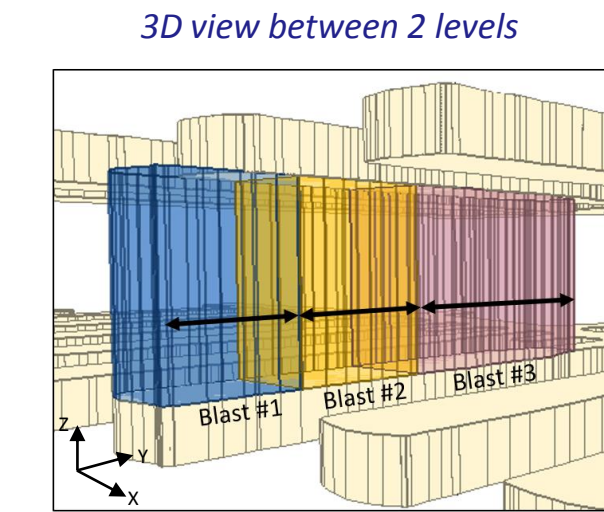
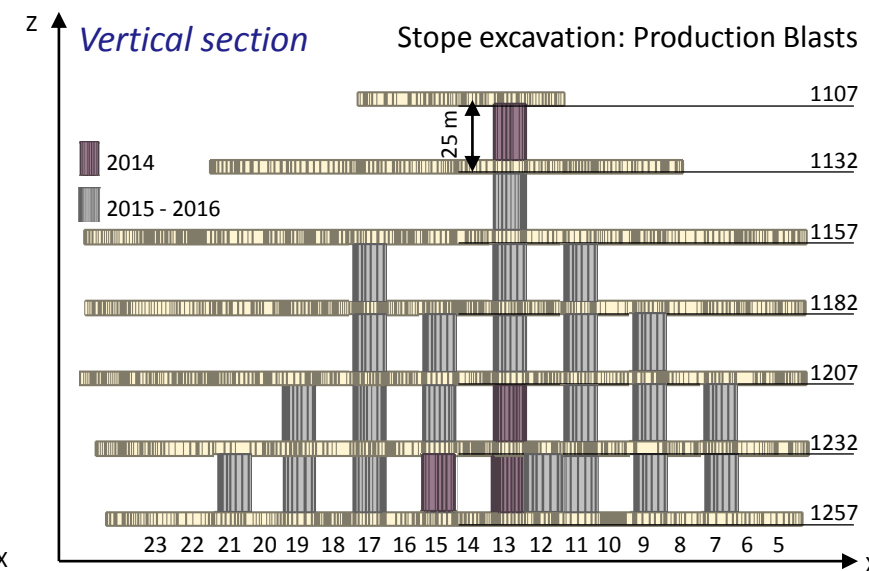
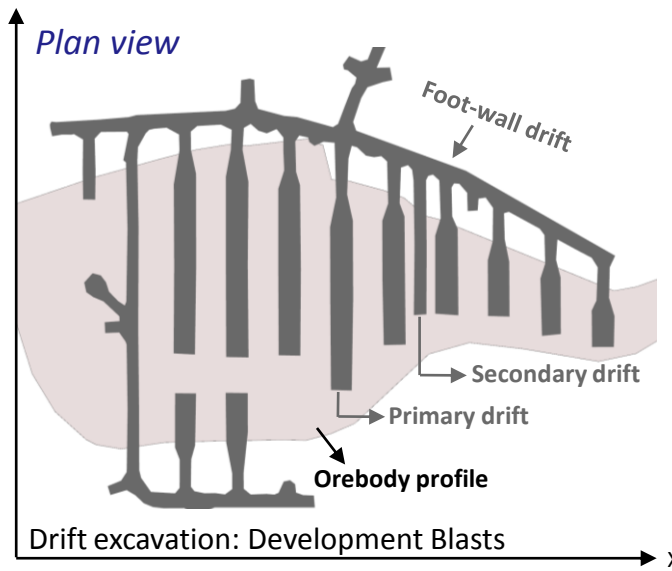


*Microseismic  
monitoring*

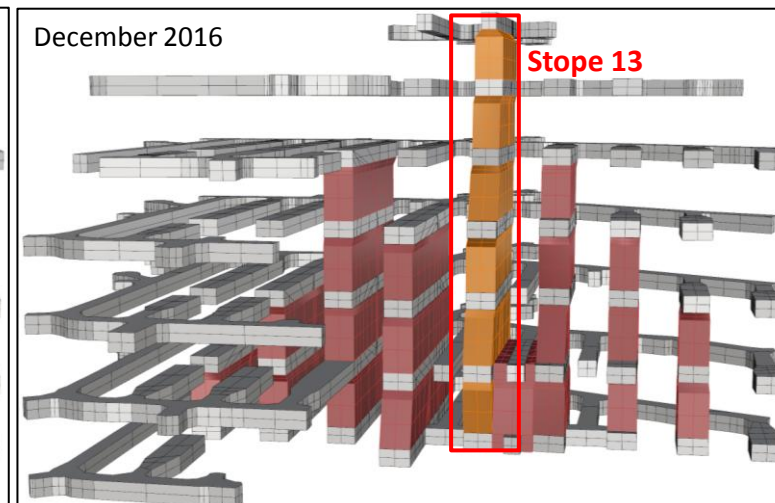
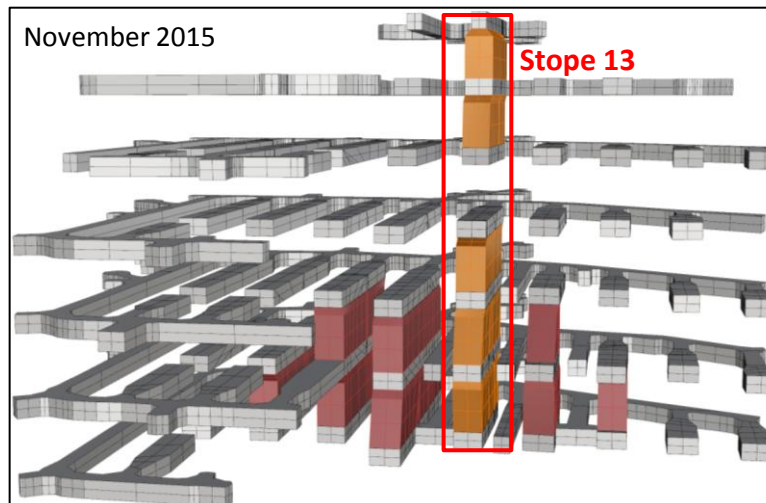
# Lappberget orebody

## Mining method and sequence

*Sublevel stoping method with backfilling*

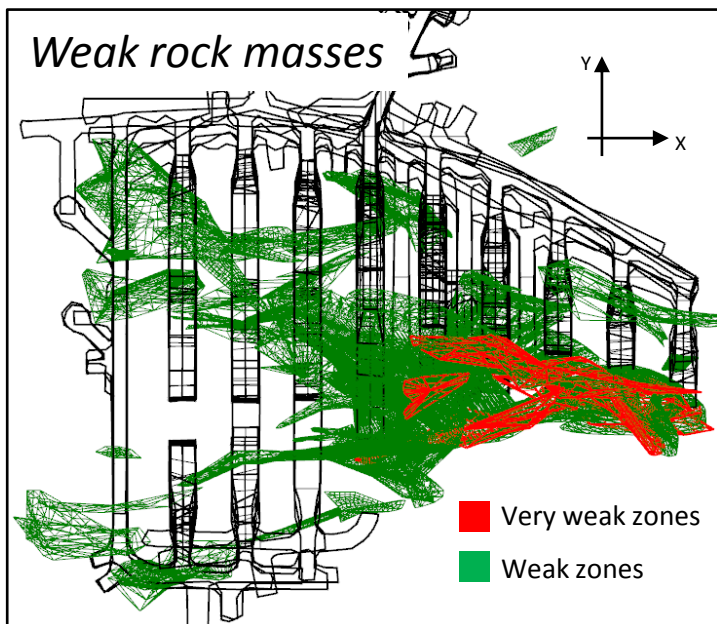
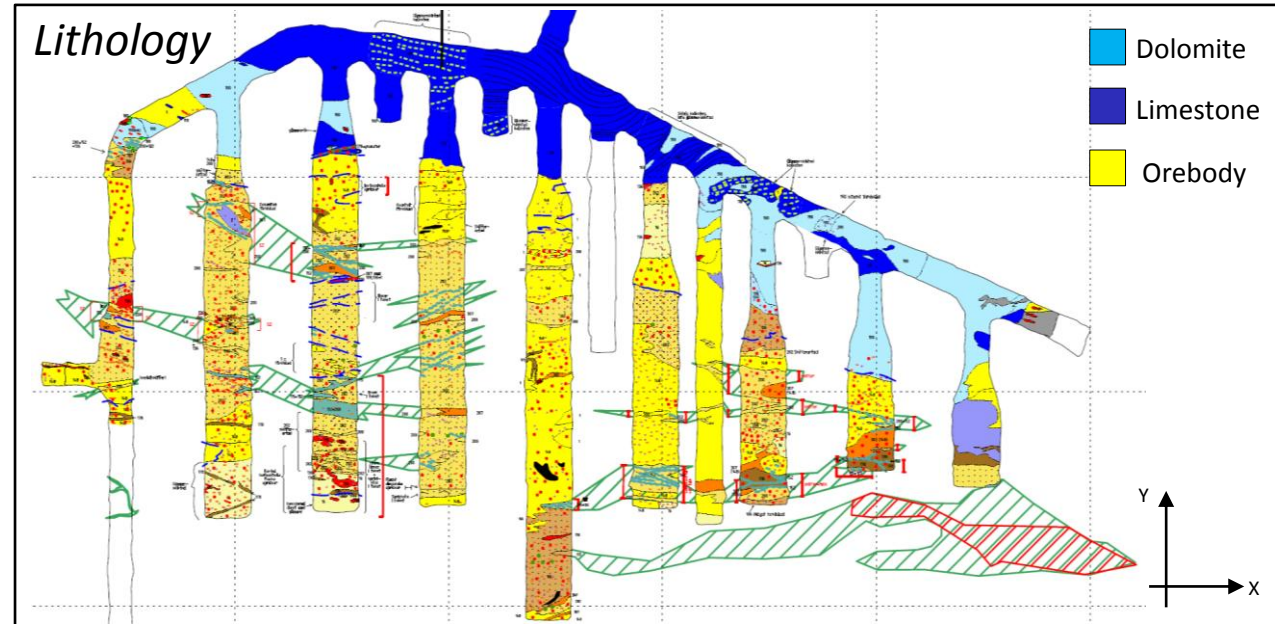
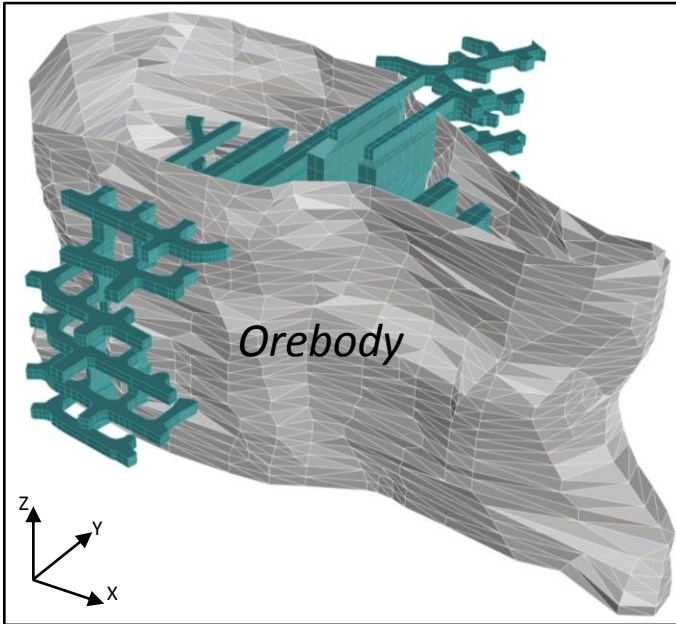


### Mining sequence



# Lappberget orebody

## Local geology



### Mechanical properties

Materials	Young modulus $E$ [MPa]	Poisson's ratio $\nu$	Density $\rho$ [kg/m <sup>3</sup> ]
Ore	66000	0.2	3030
Limestone	57000	0.18	
Weak	20000	0.3	
Very weak	2000	0.4	

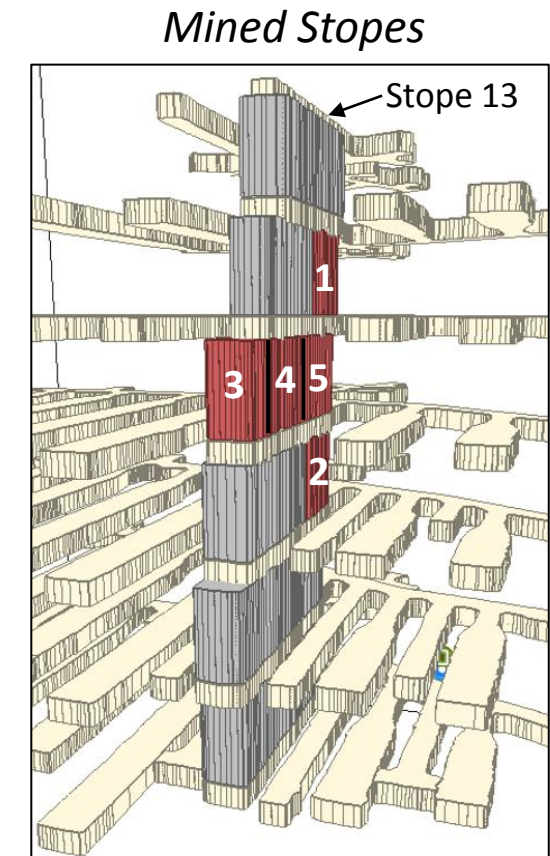
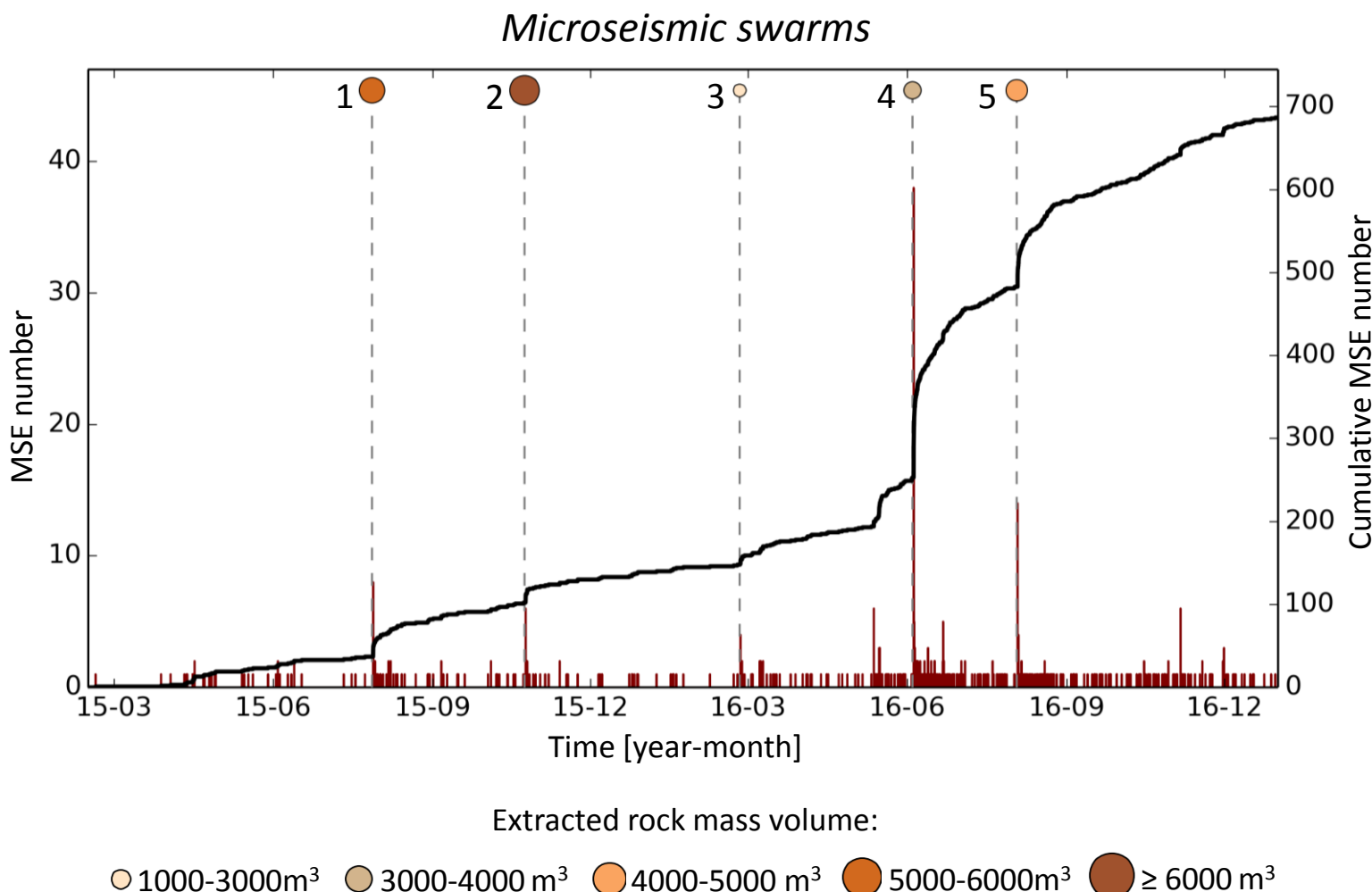
### Lack of data:

- Characteristics of fractures, joints or faults
- Mechanical properties of rock types
- No 3D information except for the orebody

# *Analysis of Lappberget Microseismic Activity between 2015 and 2016*

# Mining Production & Microseismic Activity

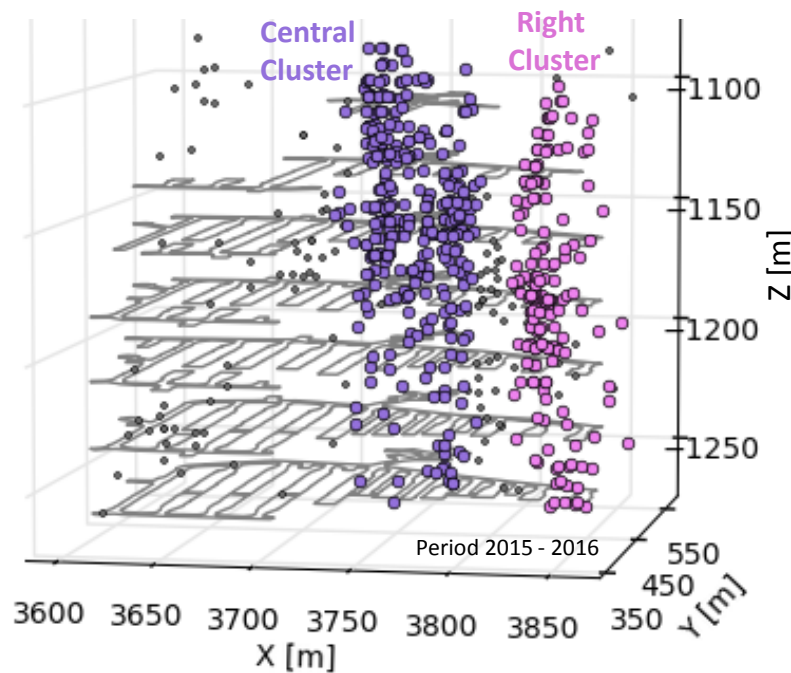
## Space-time distribution



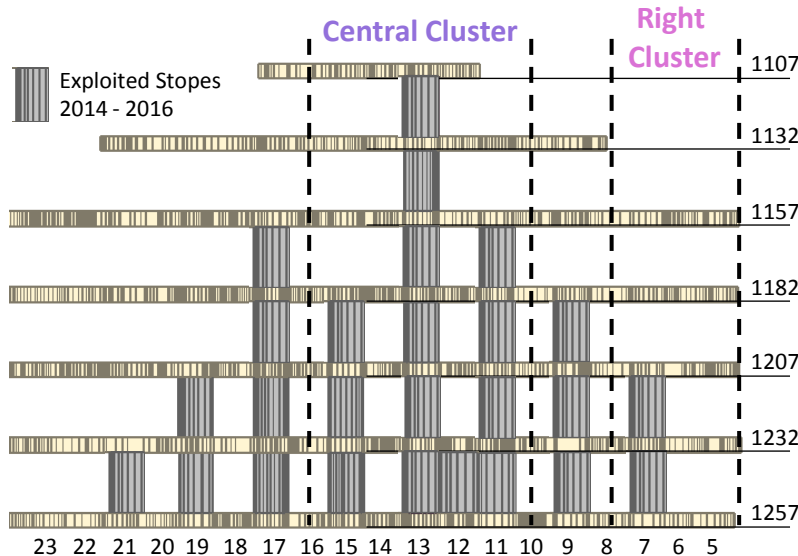
# Mining Production & Microseismic Activity

## Cluster of MSE

*Microseismic activity*

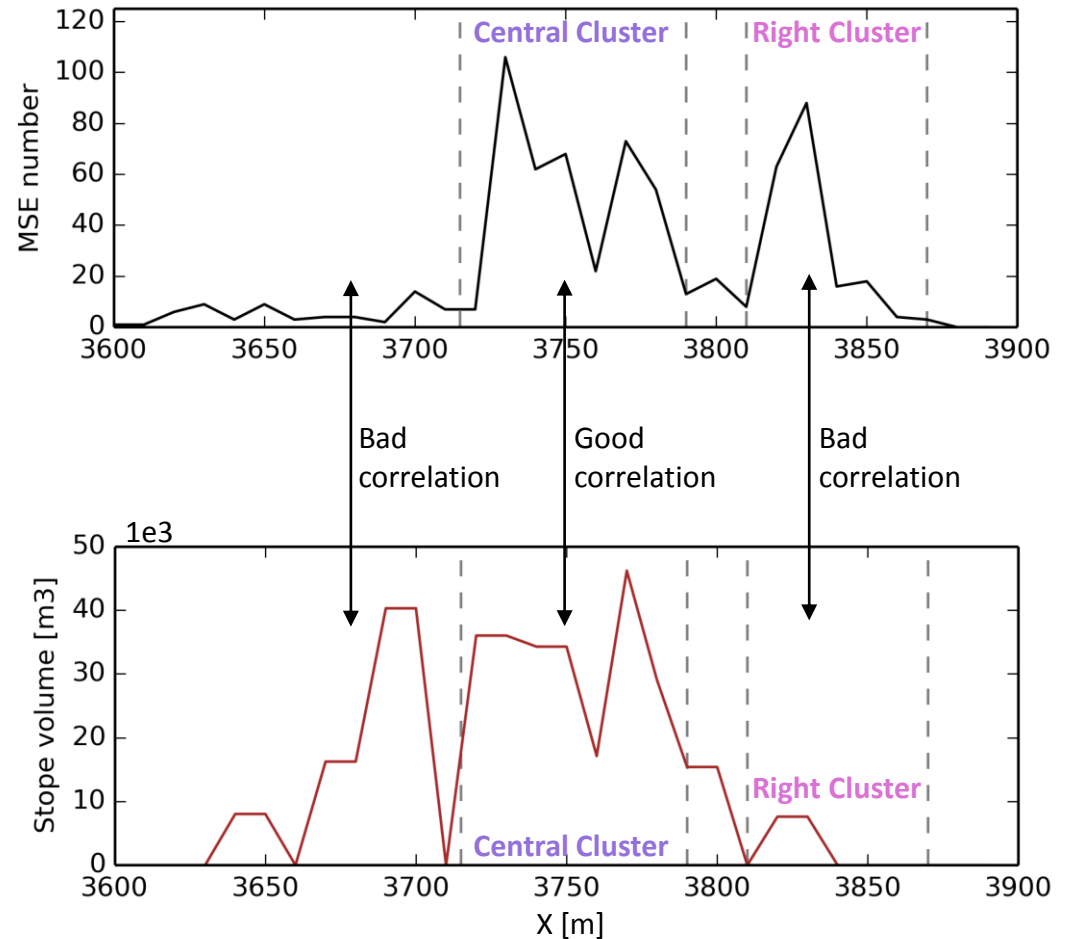


*Mine production*



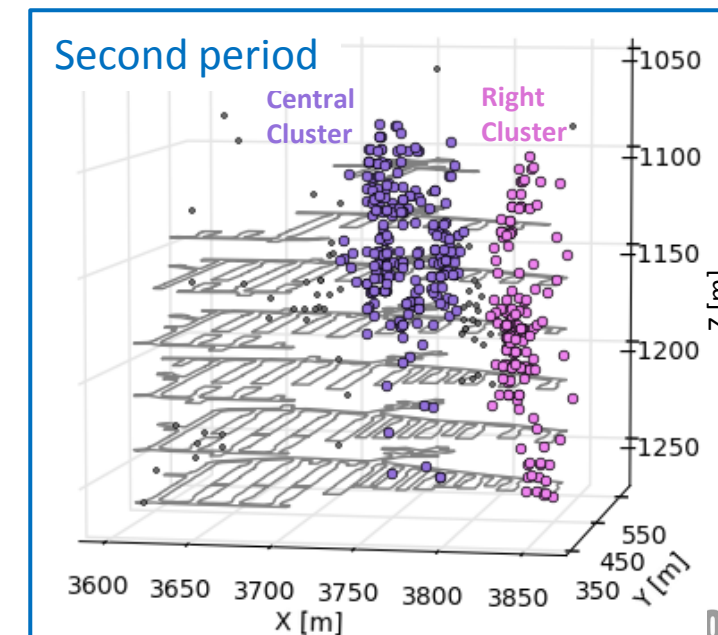
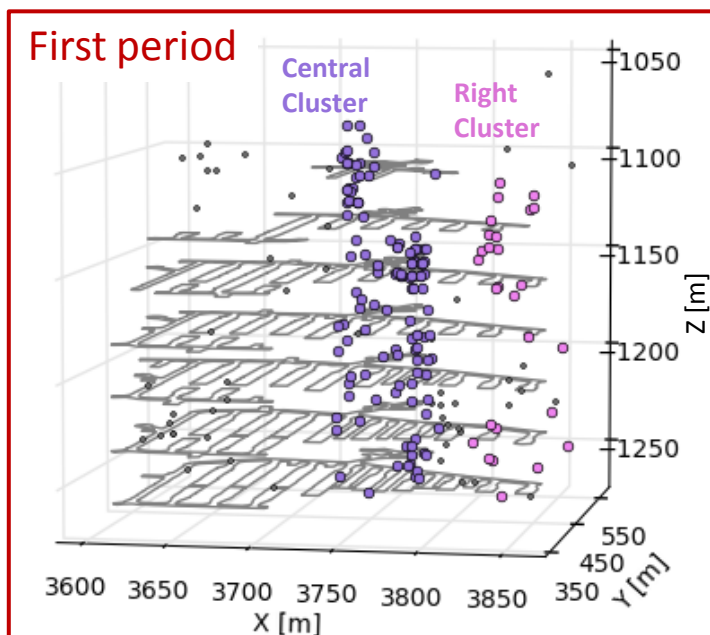
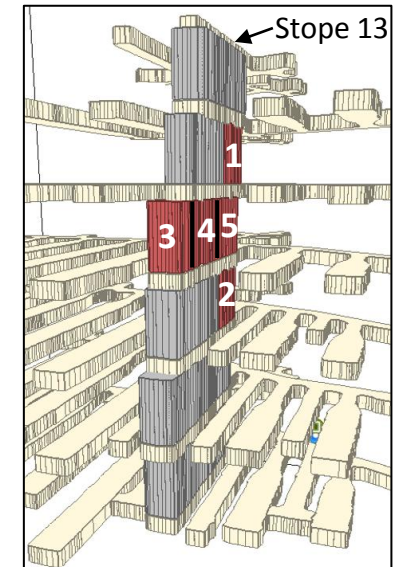
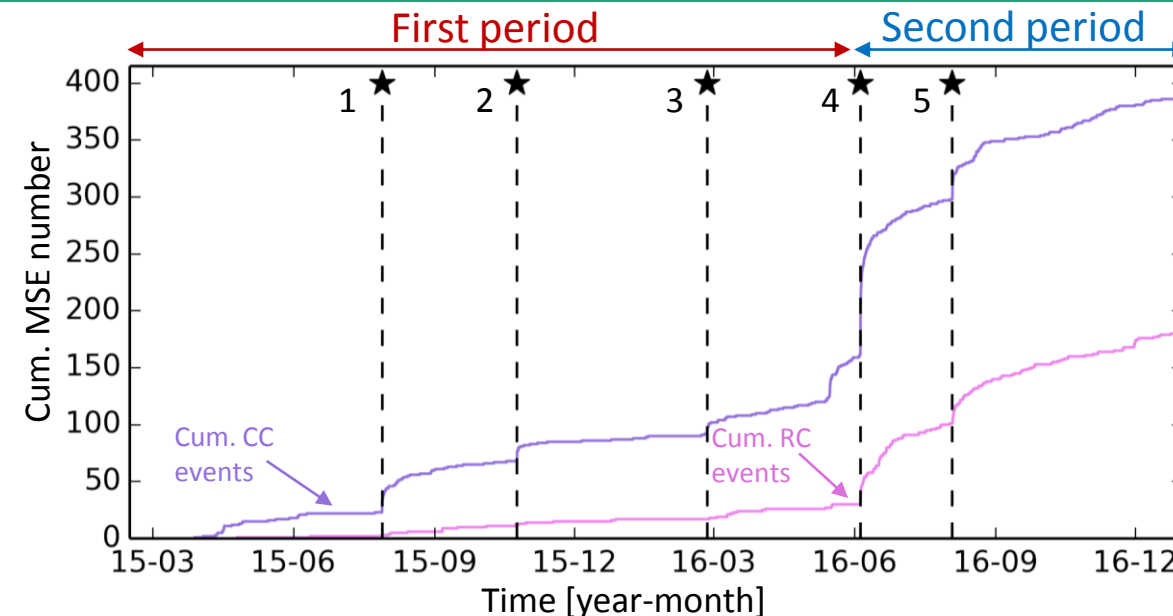
9

*MSE number & stopes volumes on a sliding window along X direction*



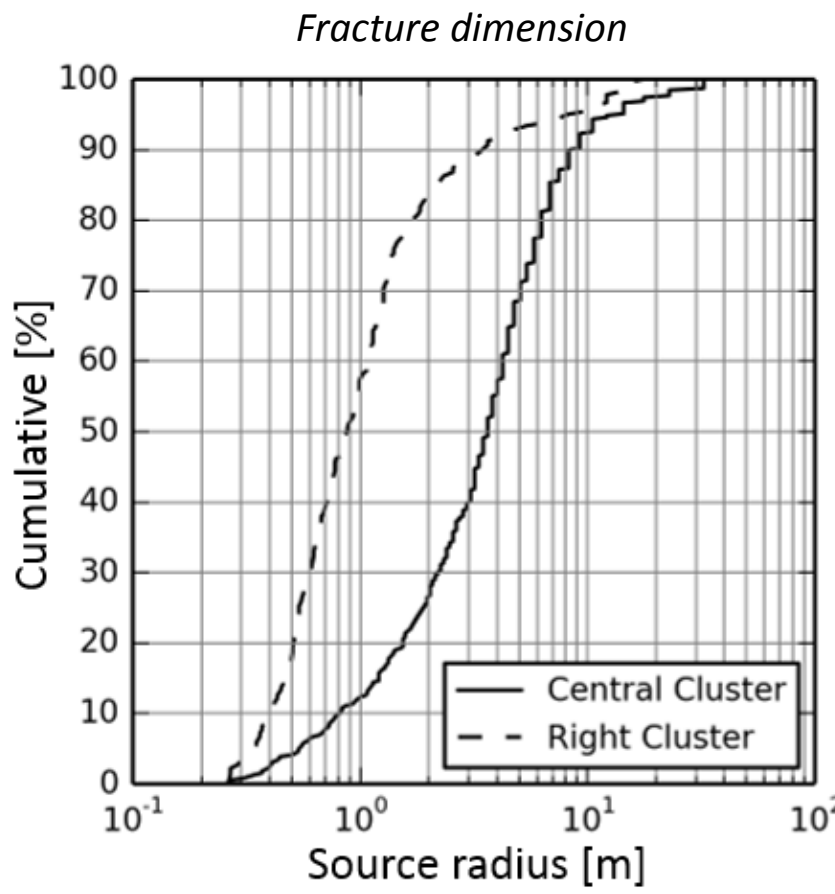
# Mining Production & Microseismic Activity

## Cluster of MSE



# Seismic source characteristics

## Fracture size and Apparent Stress

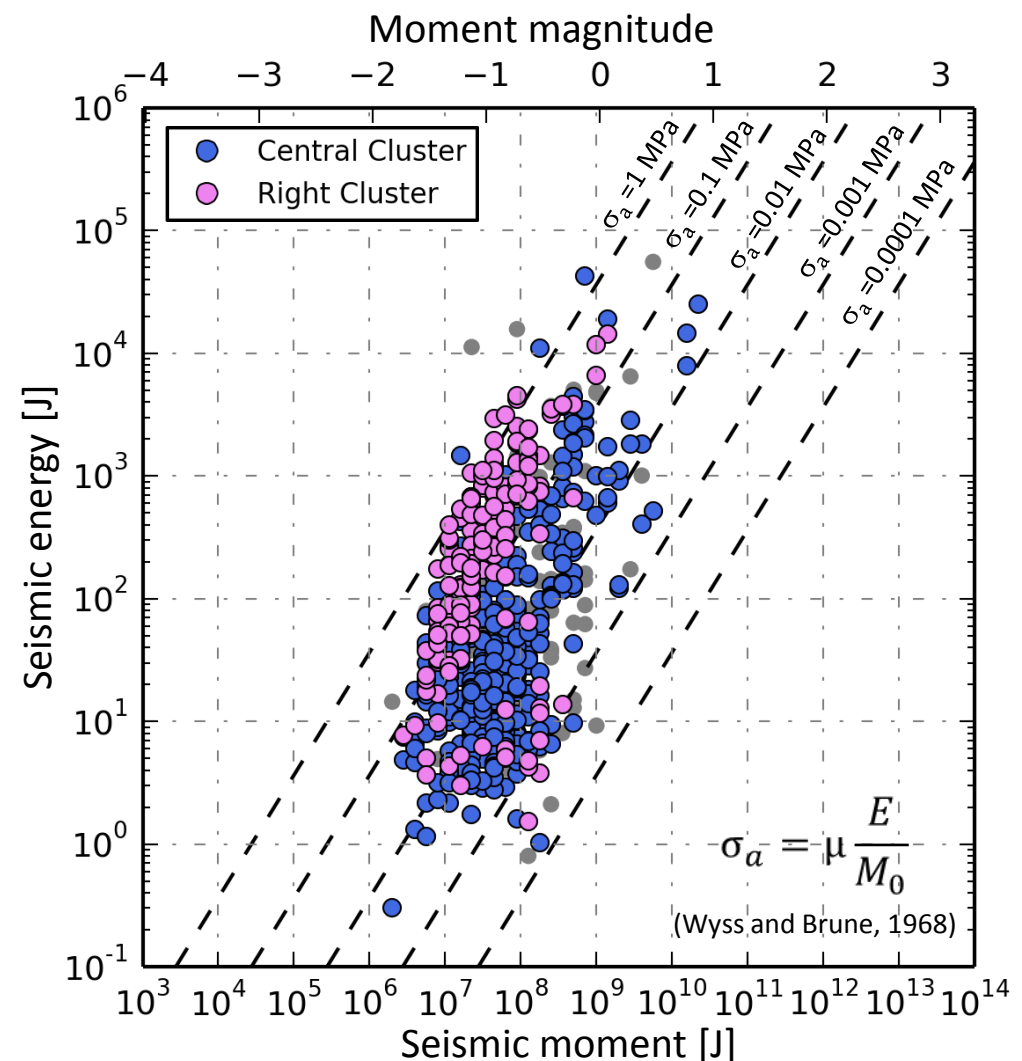


$$f_c = k_c \frac{V_S}{r} \quad k_c = \text{constant [-]}$$

$r = \text{source radius [m]}$

$V_S = S \text{ wave velocity [m/s]}$

- Source radius ⇒ from 0.3 m up to 32 m
- Median RC radius = 0.9 m
- Median CC radius = 3 m



- Apparent stress ⇒ measure of stress release at a seismic source
- Bigger stresses in the Right Cluster area

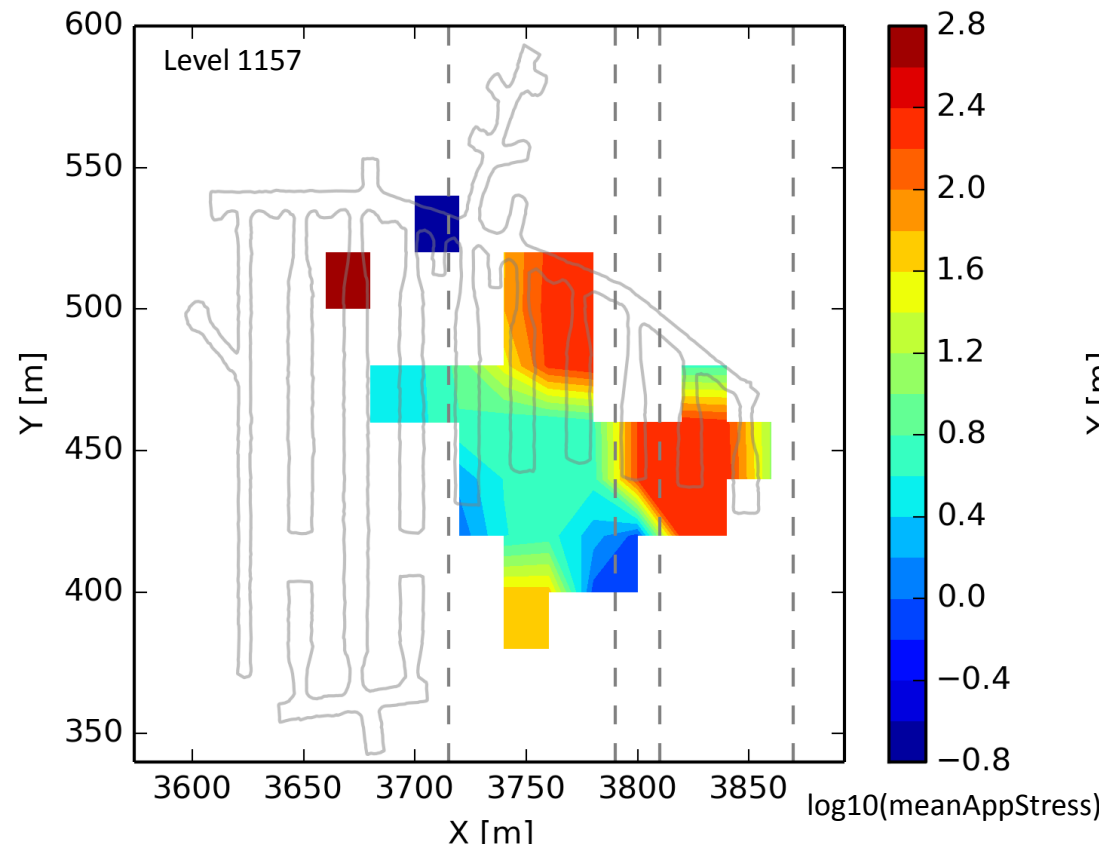
# Seismic source characteristics

## Apparent stress

Contour maps of apparent stress

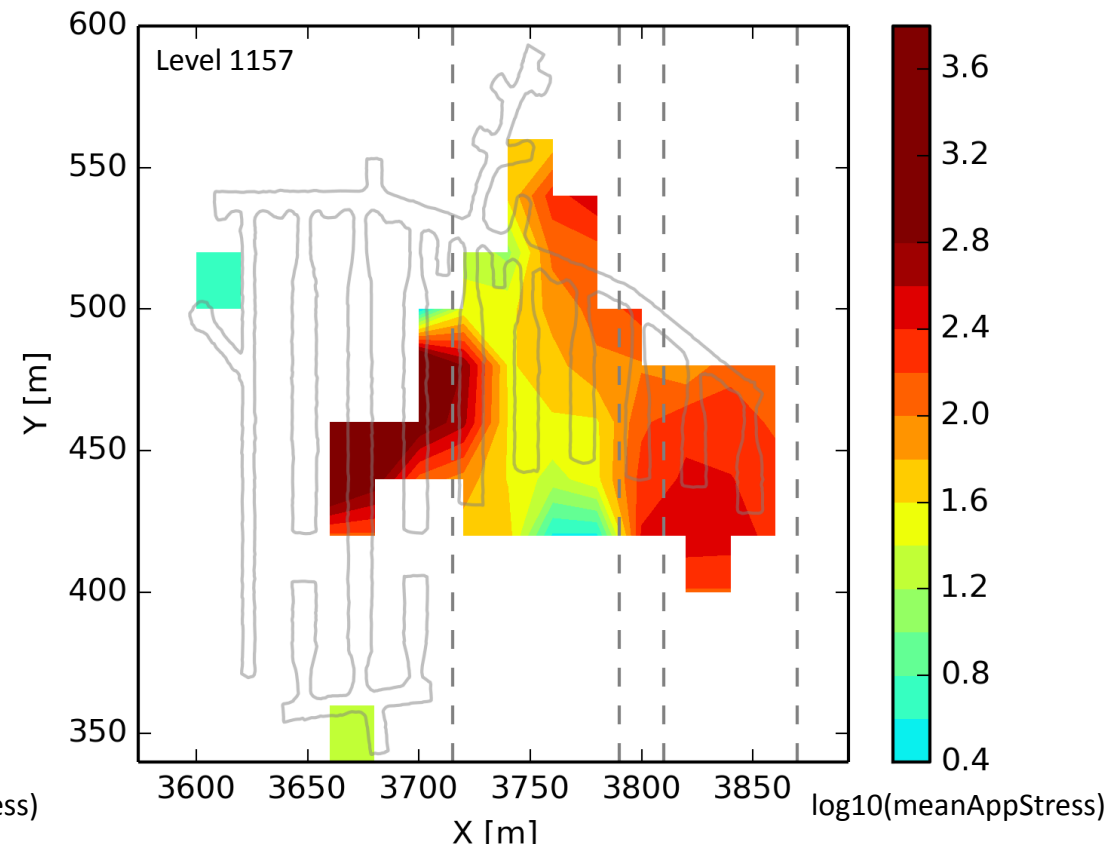
### First period

February 2015 - May 2016



### Second period

June 2016 - December 2016



# Conclusions on seismic data analysis

Central Cluster	Right Cluster
In agreement with production in the area	Linked with remote blasting in stope 13
Active since the beginning of the monitoring	Activated at final stages of stope 13 exploitation + Influenced by local geology
Bigger fractures	Smaller fractures
Lower apparent stress values	High apparent stress values



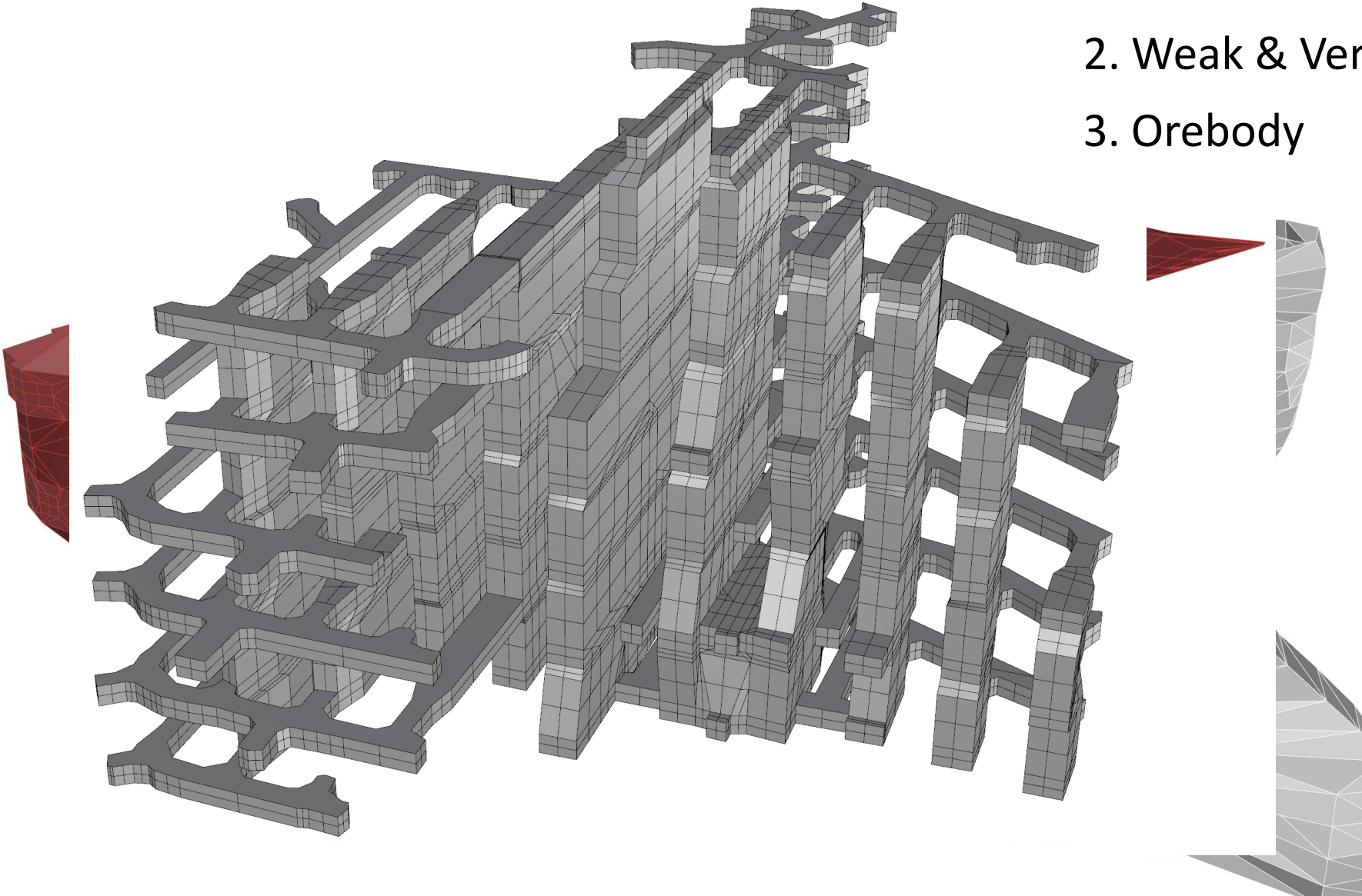
# *Numerical Modelling*

## *Simulation of the exact mine sequence between 2015 and 2016*

# Numerical Model

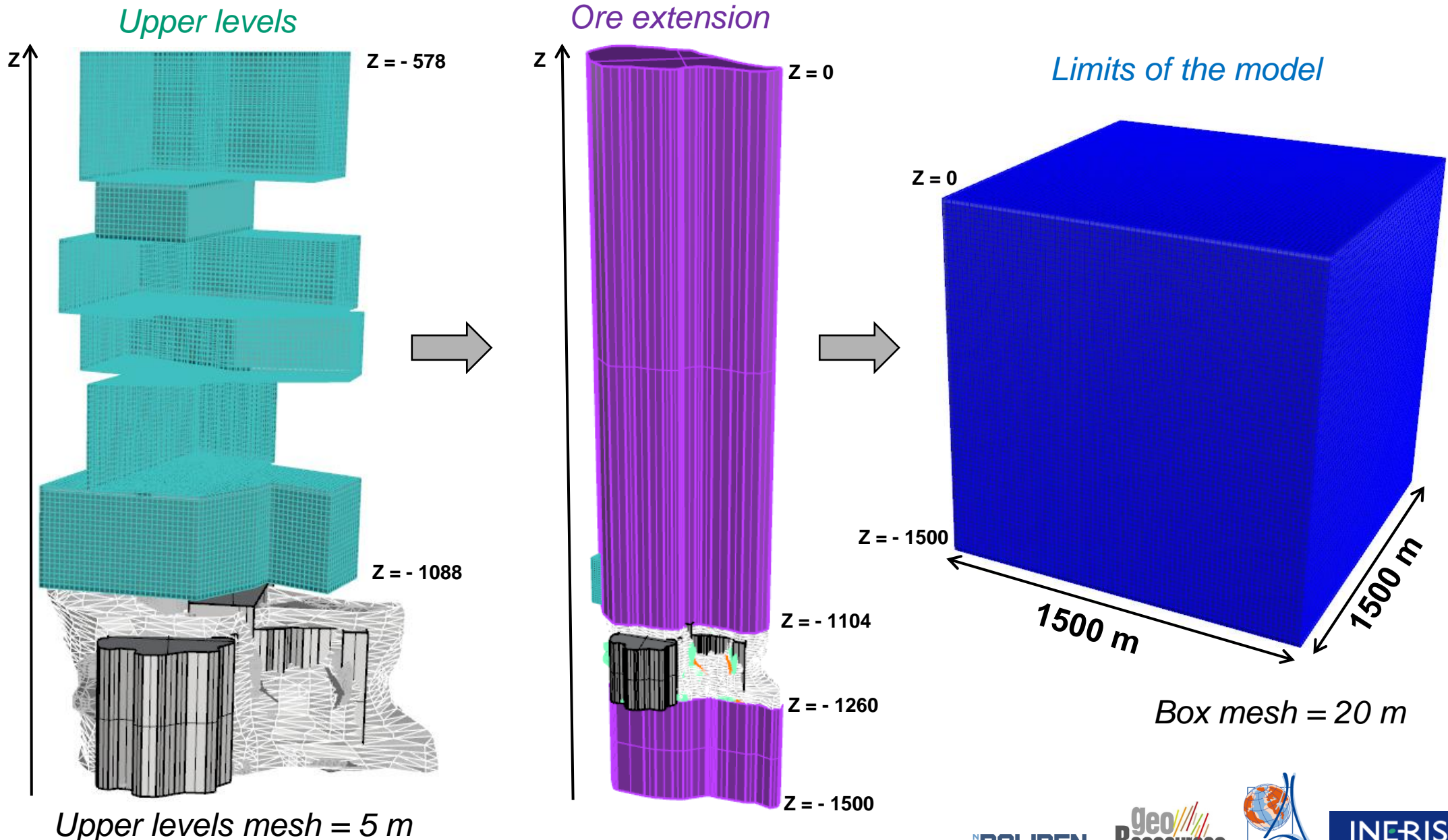
## Geometry & Meshing

1. Galleries & Stopes
2. Weak & Very weak zones
3. Orebody



# Numerical Model

## Geometry & Meshing



# Numerical Model

## Boundary Conditions & Mechanical Parameters

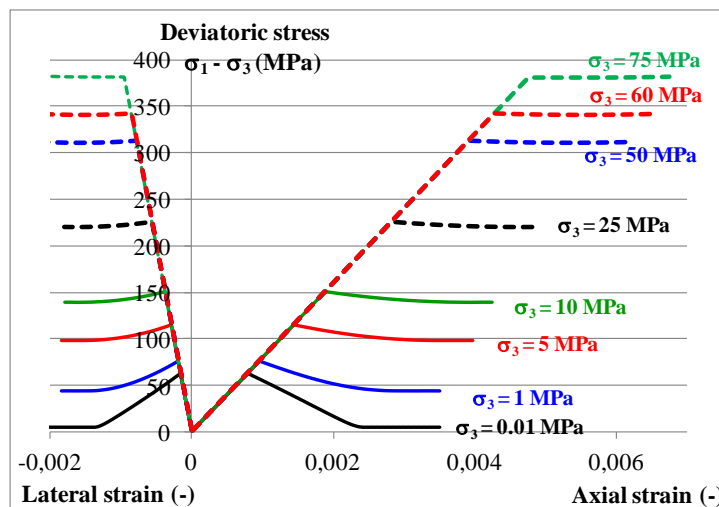
### Initials & Boundary Conditions

$$\sigma = f(z) = \rho g \begin{pmatrix} k_X \\ k_Y \\ 1 \end{pmatrix} z \quad \left\{ \begin{array}{l} \sigma_X = 44.3 \text{ MPa} \\ \sigma_Y = 47.3 \text{ MPa} \\ \sigma_Z = 34 \text{ MPa} \end{array} \right.$$

### Failure criteria

Hoek-Brown failure criteria  $\Rightarrow \frac{\sigma_1}{\sigma_c} = \frac{\sigma_3}{\sigma_c} + \sqrt{m \frac{\sigma_3}{\sigma_c} + s}$

### Brittle failure criteria



(Souley et al., 2018)

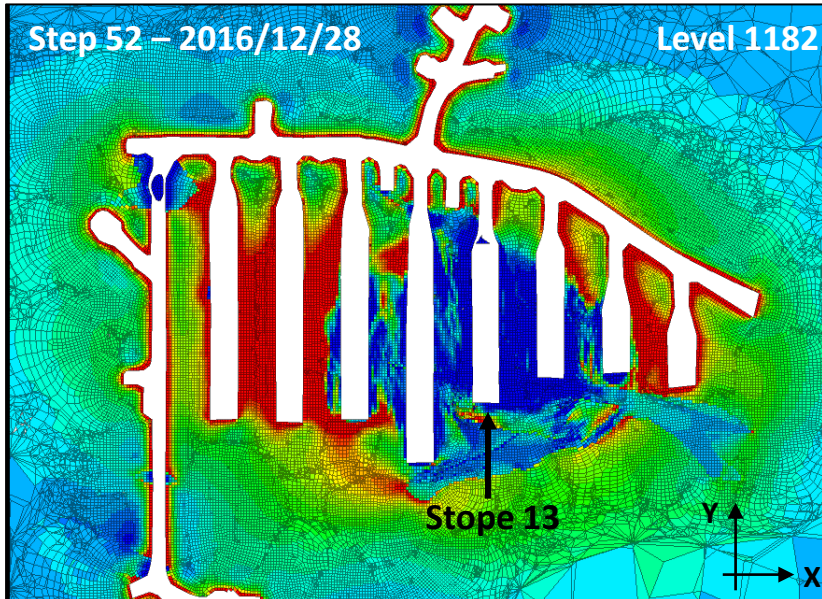
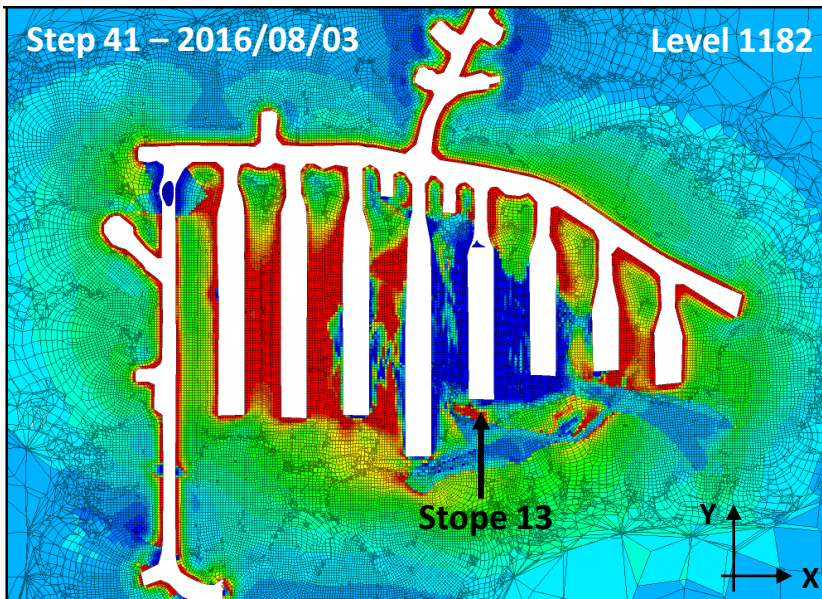
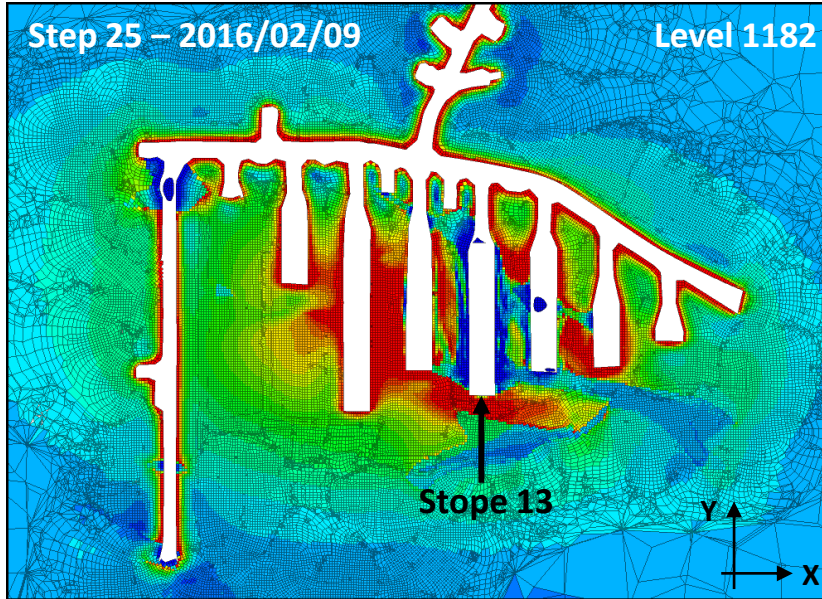
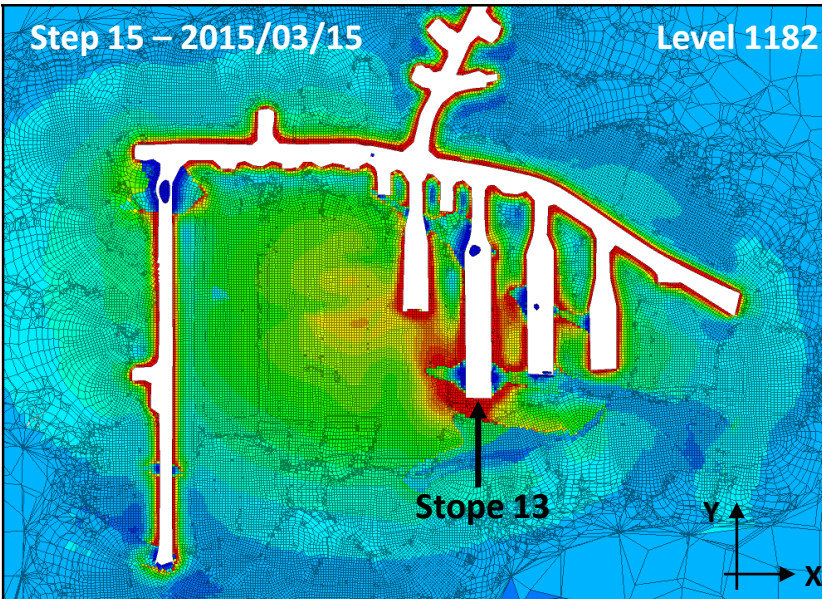
Materials	Elastic parameters		Hoek-Brown parameters			Density $\rho$ [kg/m³]
	Young modulus E [MPa]	Poisson's ratio $\nu$	$m$	$s$	$\sigma_c$ [MPa]	
Ore	66000	0.2	10	0.112	188	3030
Limestone	57000	0.18	10	0.112	110	
Weak	20000	0.3	1	0.001	30	
Very weak	2000	0.4	0.63	0.00024	10	
Paste	500	0.2	-	-	-	

### Brittle failure criteria parameters

Materials	$m_r$	$\sigma_3^{b-d}$	$s_r$	$\xi_r$	$\beta_m$	$b_1$
Ore	2	$\sigma_c * (s)^{1/2}$	$s * 1e-5$	0.0025	$\tan(15^\circ)$	750

# Numerical Model

## Model Results



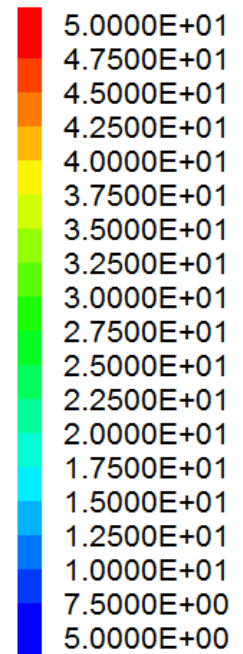
$$q^{ini} = 12.1 \text{ MPa}$$

$$\sigma_x^{ini} = 44.3 \text{ MPa}$$

$$\sigma_y^{ini} = 47.3 \text{ MPa}$$

$$\sigma_z^{ini} = 34 \text{ MPa}$$

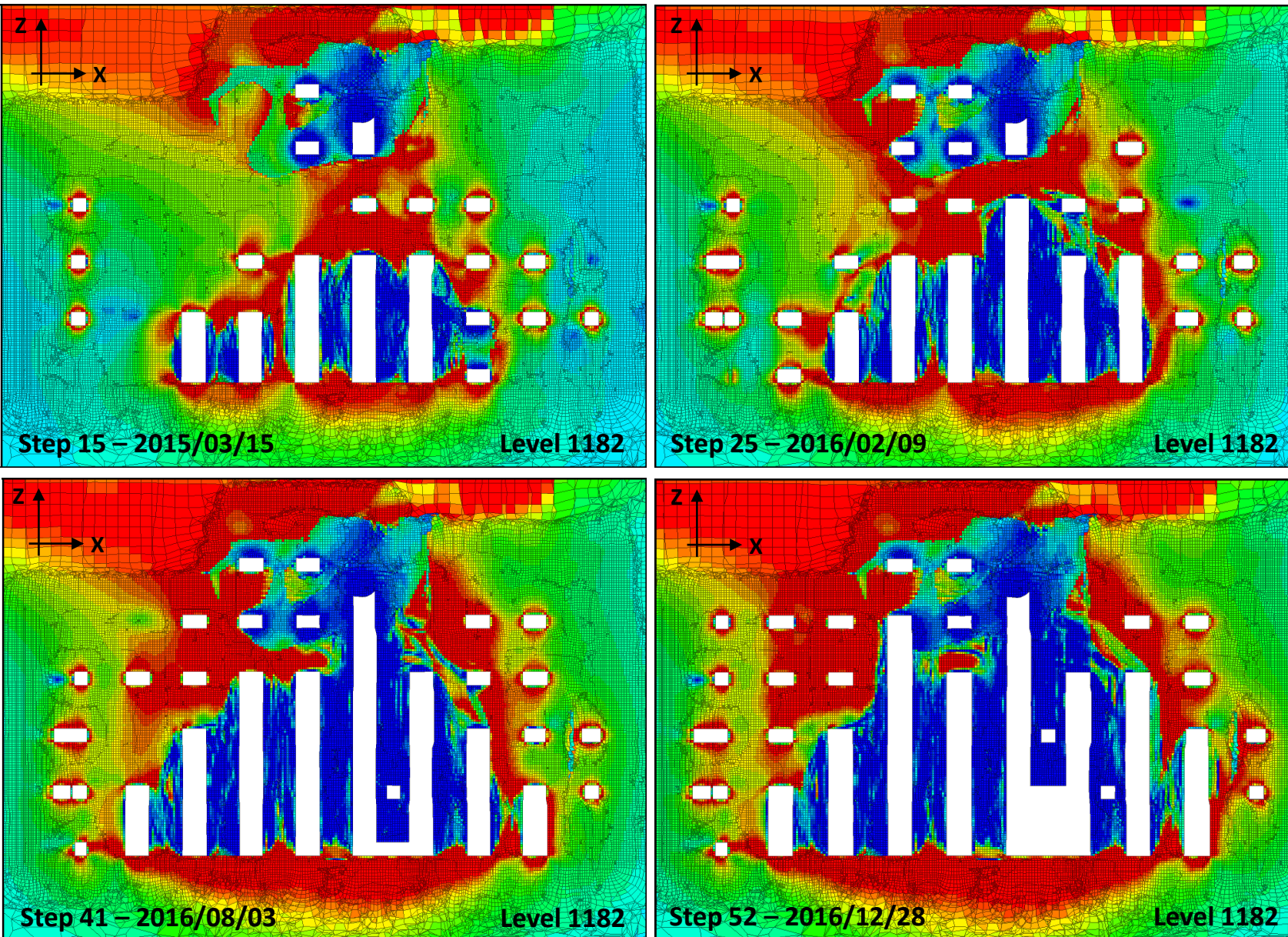
Deviatoric stress \* [MPa]



$$* q = \sqrt{3J_2} = \sqrt{\frac{1}{2}[(\sigma_1 - \sigma_2)^2 + (\sigma_1 - \sigma_3)^2 + (\sigma_3 - \sigma_2)^2]}$$

# Numerical Model

## Model Results



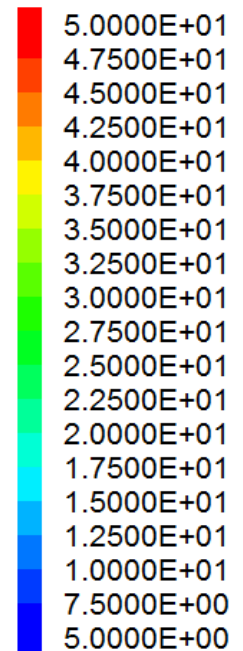
$$q^{ini} = 12.1 \text{ MPa}$$

$$\sigma_x^{ini} = 44.3 \text{ MPa}$$

$$\sigma_y^{ini} = 47.3 \text{ MPa}$$

$$\sigma_z^{ini} = 34 \text{ MPa}$$

Deviatoric stress \* [MPa]



# *Seismic Data and Model Data comparison*

# Seismic Data & Model Data

1<sup>st</sup> approach of comparison: individual measures

## Seismic parameters

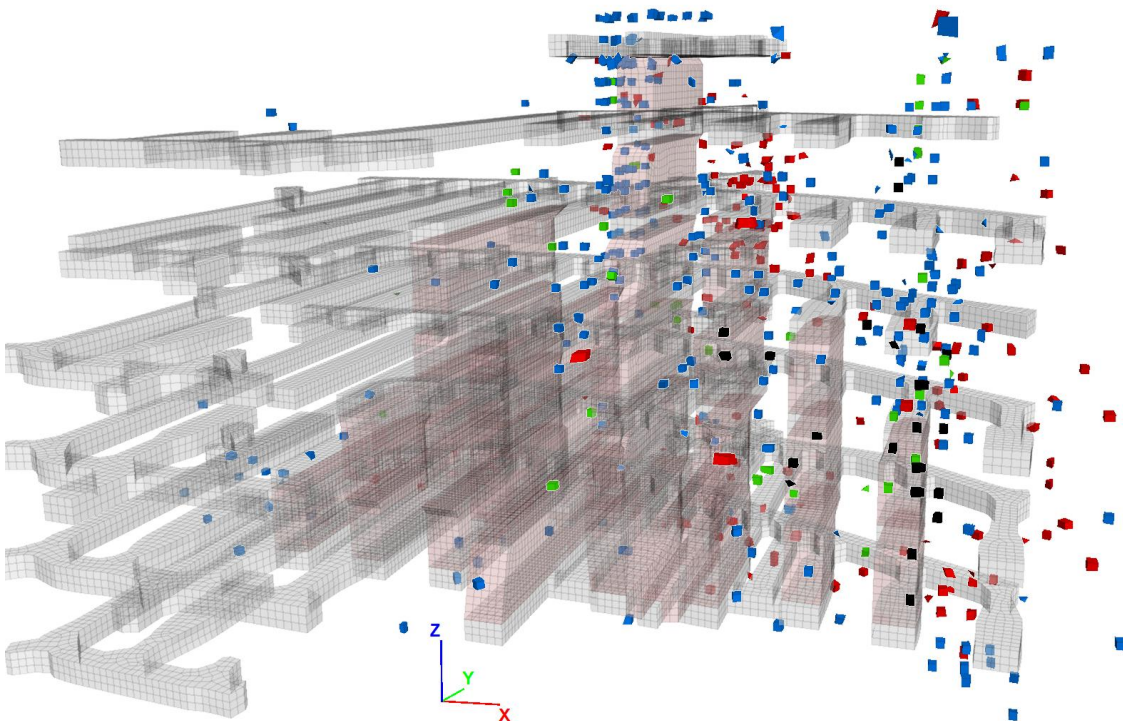
Punctual measures at seismic events locations

## Model parameters

Measures within the whole space



Model parameters calculated inside meshes at the position of MSE location



## Seismic parameters

E – seismic energy

$M_0$  – seismic moment

$M_w$  – moment magnitude

$f_c$  – corner frequency

$\sigma_{app}$  – apparent stress

$V_{app}$  – apparent volume

$\Delta\sigma$  – stress drop

## Model parameters

Stress variables

$\sigma_1$  – max. principal stress

$\sigma_2$  – inter. principal stress

$\sigma_3$  – min. principal stress

$\sigma_{ij}$  – stress tensor

$\varepsilon_q$  – Von Mises stress

Strain variables

$\varepsilon_1$  – max. principal strain

$\varepsilon_2$  – inter. principal strain

$\varepsilon_3$  – min. principal strain

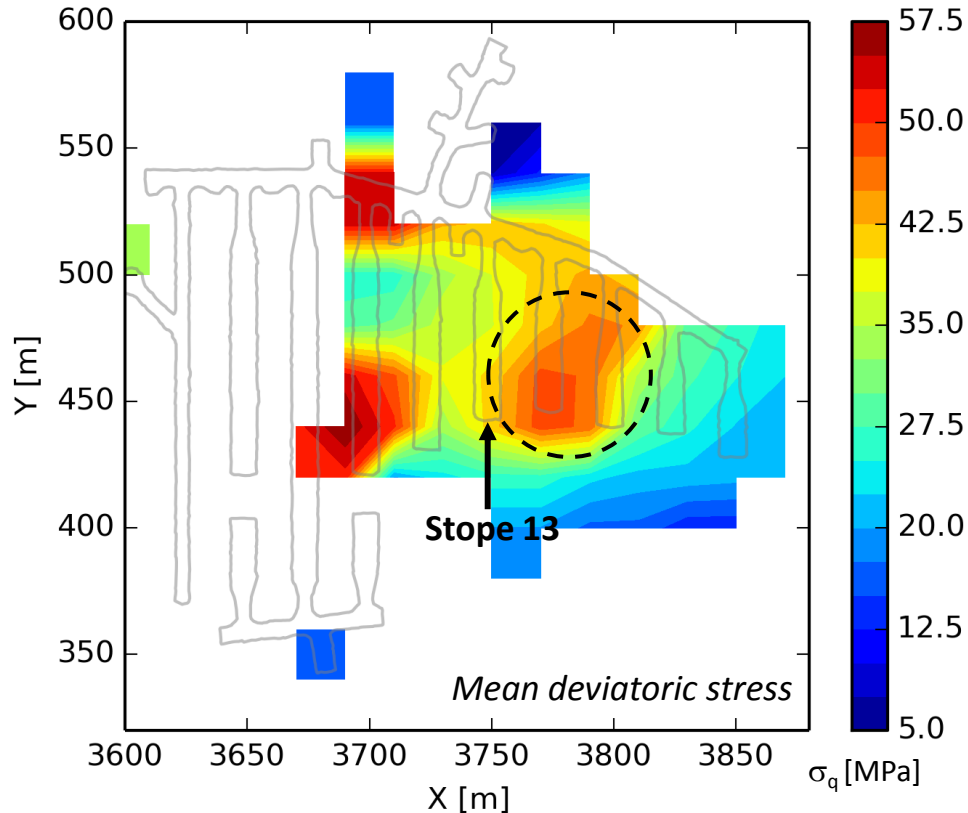
$\varepsilon_{ij}$  – strain tensor

$\varepsilon_q$  – Von Mises strain

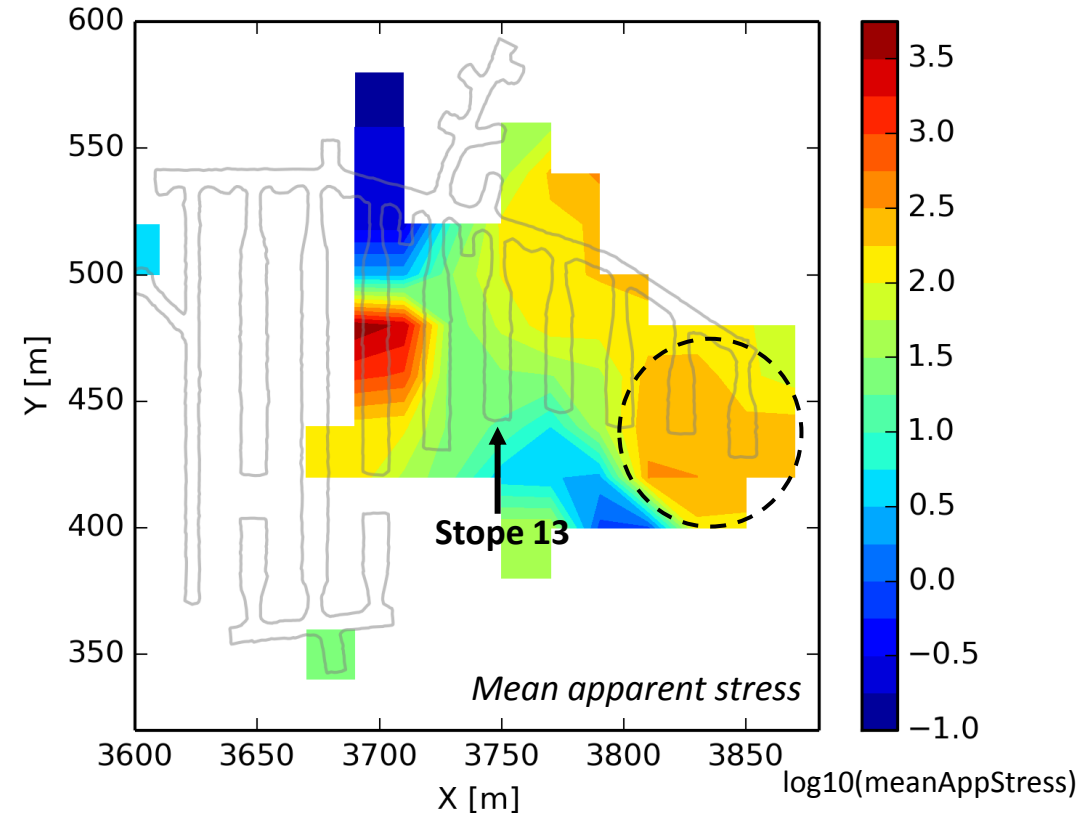
# Seismic Data & Model Data

## Qualitative Analysis

*Model parameter*

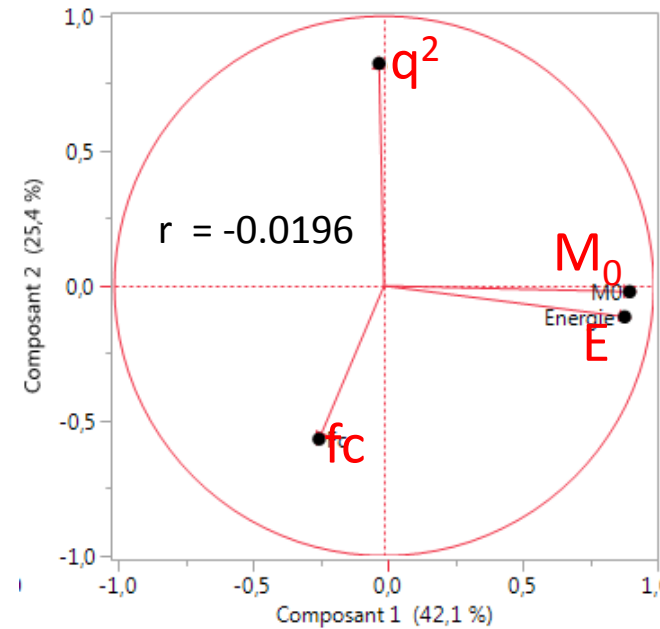
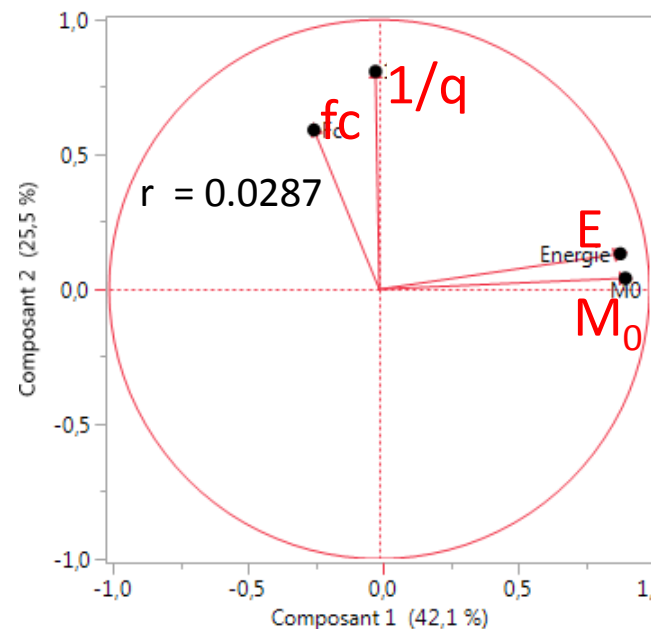
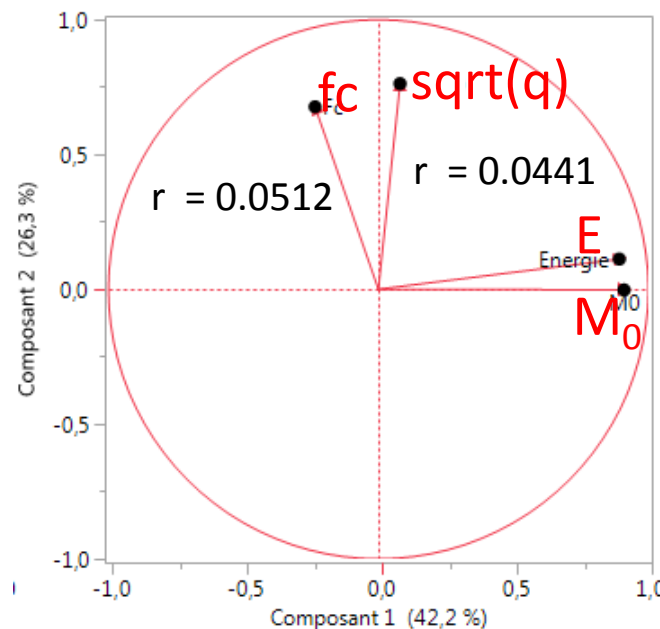
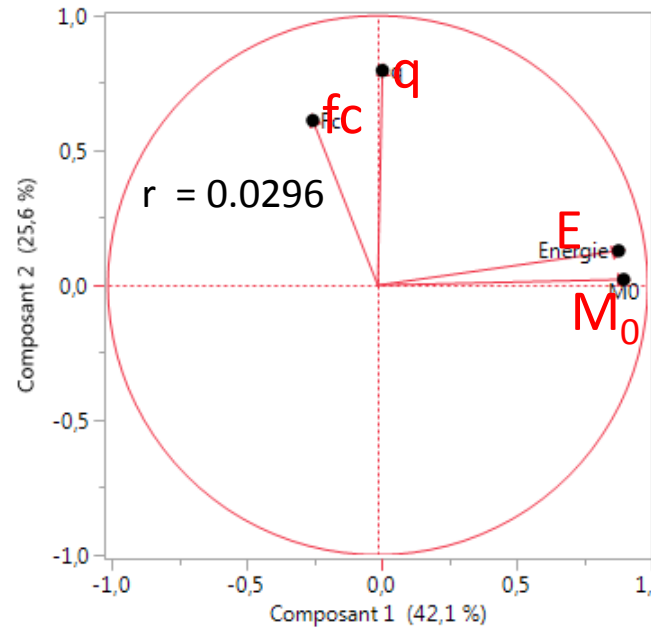


*Seismic parameter*



# Seismic Data & Model Data

## Quantitative Analysis: Principal Component Analysis



# Seismic Data & Model Data

2<sup>nd</sup> approach of comparison: cumulated measures

## Seismic parameters

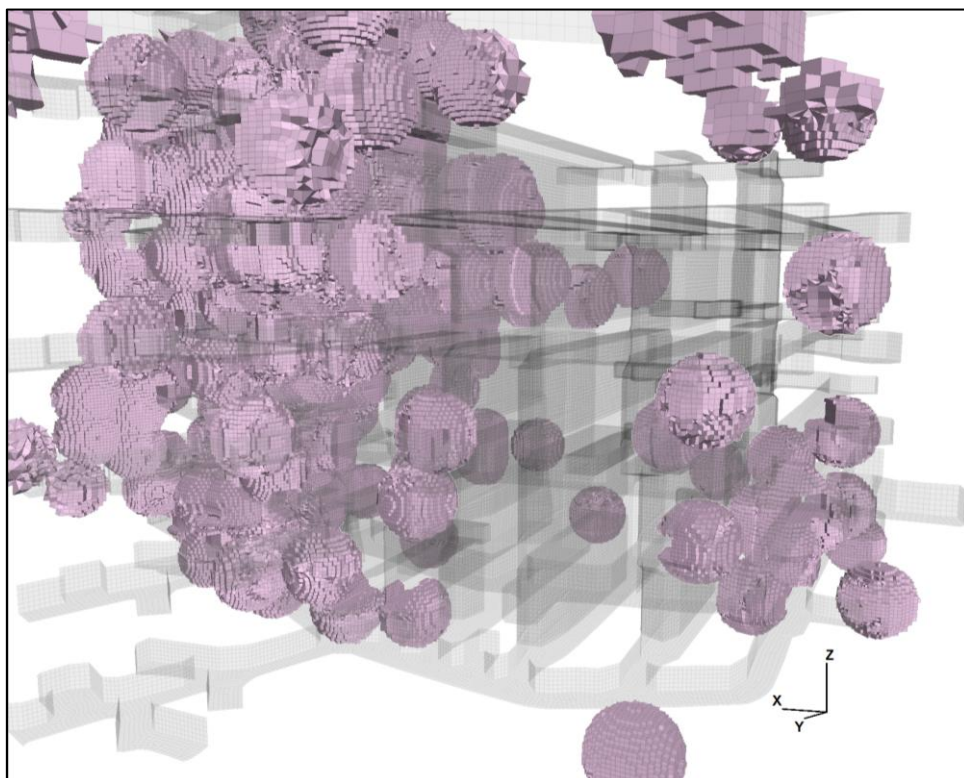
Punctual measures at seismic events locations

## Model parameters

Measures within the whole space



Cumulated model parameters calculated inside the spheres of 10 m radius around each seismic events location



## Seismic parameters

E – seismic energy

$M_0$  – seismic moment

$V_a$  – max. principal stress

$A_s$  – Source area

## Model parameters

Elastic

Plastic

Volumetric elastic energy

Volumetric plastic energy

Shear elastic energy

Shear plastic energy

Total elastic energy

Total plastic energy

Plastic volume

Mean Von Mises stress and strain

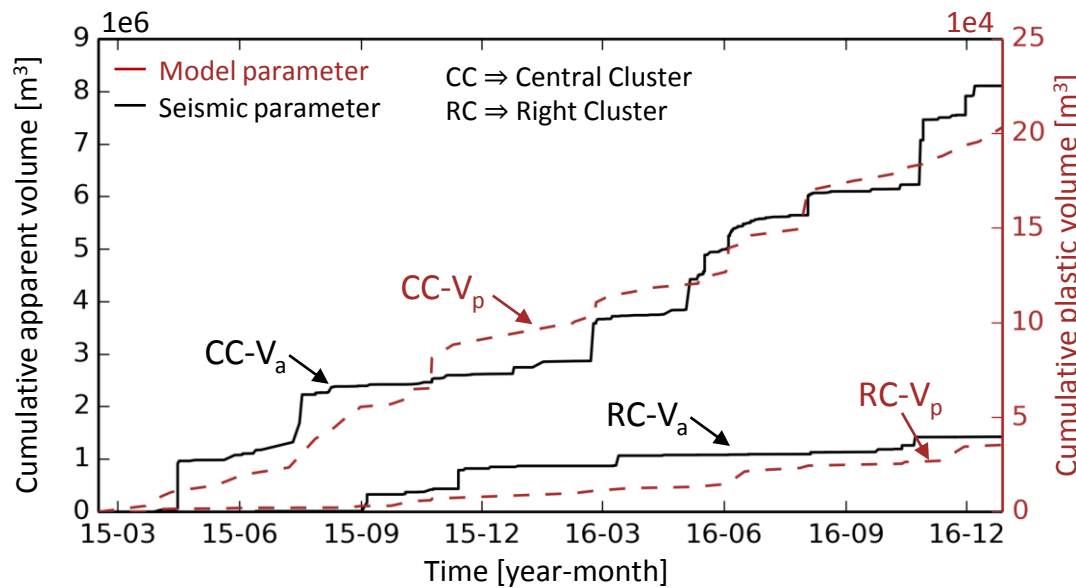
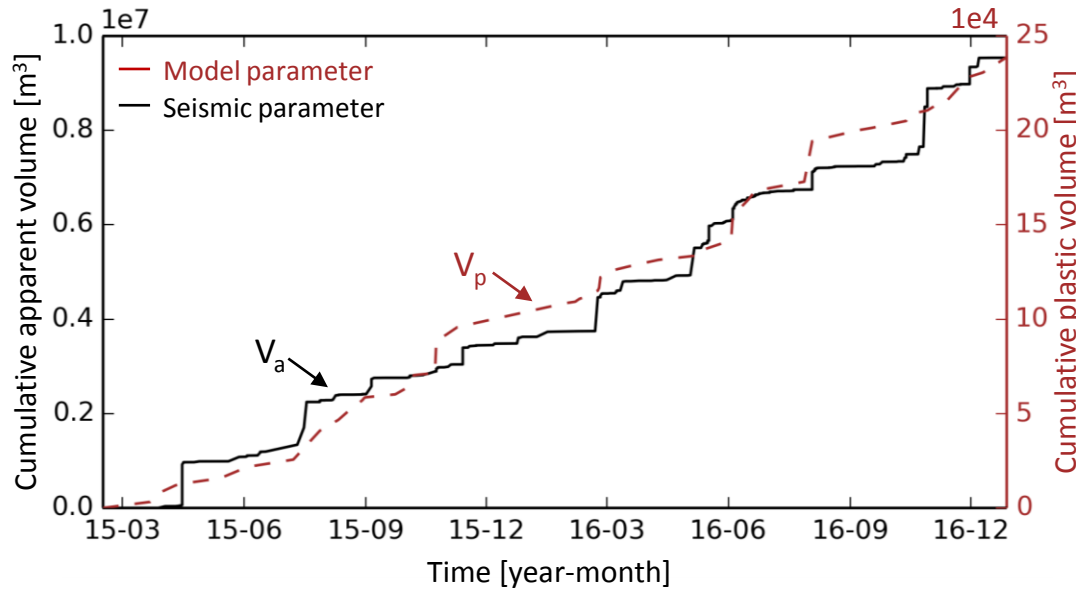
Mean of max. shear strain

Volumetric strain

Shear strain

# Seismic Data & Model Data

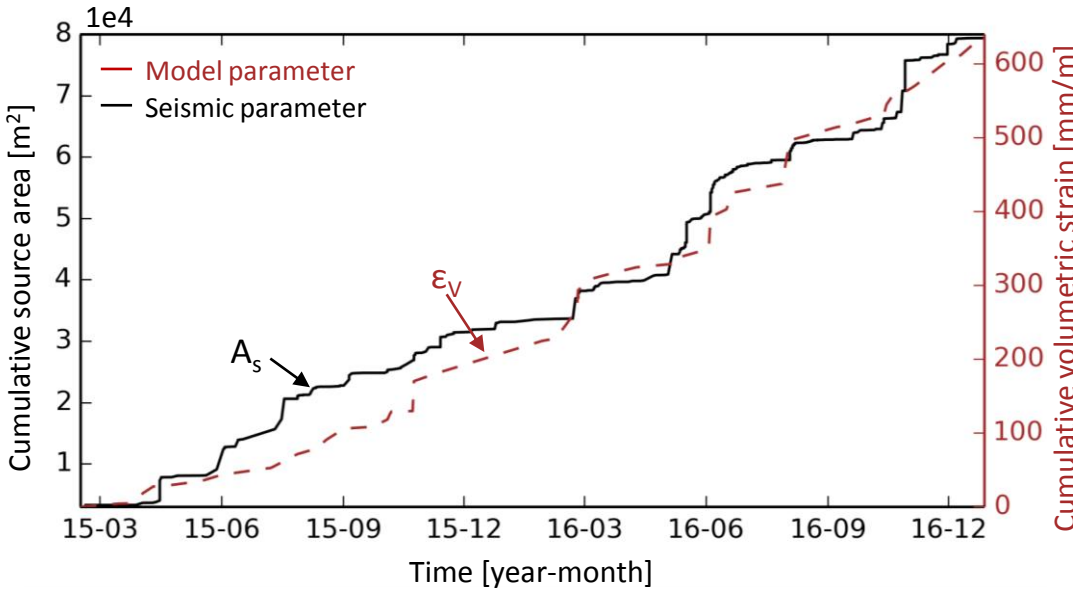
## Qualitative Analysis



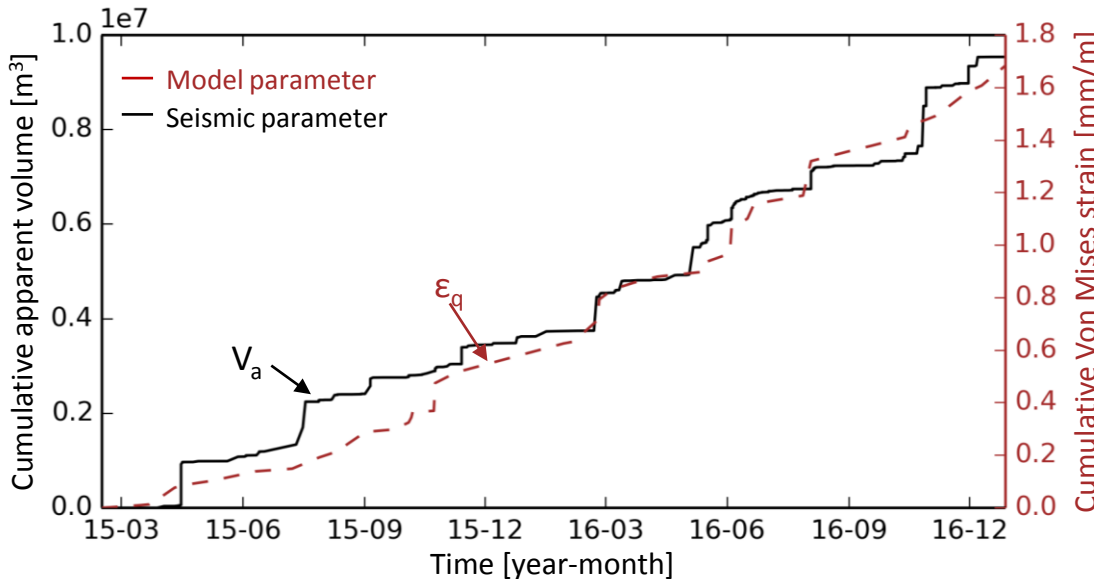
$$\left. \begin{array}{l} \text{Apparent volume} \Rightarrow V_a = \frac{M_0^2}{2\mu E} [\text{m}^3] \\ \text{Plastic volume} \Rightarrow \text{volume of plastic zones in the spheres} \end{array} \right\}$$

# Seismic Data & Model Data

## Qualitative Analysis



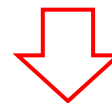
$$\left. \begin{array}{l} \text{Source area} \Rightarrow A_s = \pi r^2 [m^2] \\ r \text{ determined from } f_c = k_c \frac{V_s}{r} \\ \text{Volumetric strain} \Rightarrow t_r(\epsilon) \end{array} \right\}$$



$$\left. \begin{array}{l} \text{Apparent volume} \Rightarrow V_a = \frac{M_0^2}{2\mu E} [m^3] \\ \text{Von Mises strain} \Rightarrow \epsilon_q = \sqrt{\frac{4}{3} J_2} \end{array} \right\}$$

# Discussion and Perspectives

- Seismic & numerical model shows increasing stresses around the main production area
- Spatialization problem
  - Uncertainties in events location & model uncertainties
  - Reactivation of preexisting structure not taken into account in the model
- Cumulating seismic and numerical parameters in space correlations are improved



- Improvement of events detection and location
  - Detection: bigger number of seismometers and continuous recordings
  - Location: new location methods based on double difference and multiples analysis
- Include fractures in the model
  - Bigger fractures of CC may be modeled based on focal mechanism of MSE
  - Smaller fractures of RC cannot be included in the model with the actual mesh  
⇒ reduce mechanical properties of some meshes?
- Taking creep into account
  - Seismic swarms are long lasting in time (more than 1 month)
  - Stress measurements have shown a differential response of deformations during time

# Questions ?

## References

DeSantis, F., Contrucci, I., Lizeur, A., Tonnellier, A., Matrullo, E., Bernard, P., Nyström, A., 2017. Numerical approach for evaluating microseismic array performances: case study of a deep metal mine monitoring network, in: Proceedings of the 9th International Symposium on Rockbursts and Seismicity in Mines.

Tonnellier, A., Bouffier, C., Renaud, V., Bigarré, P., Mozaffari, S., Nyström, A., Fjellström, P., 2016. Integrating microseismic and 3D stress monitoring with numerical modeling to improve ground hazard assessment, in: Proceedings of the Eighth International Symposium on Ground Support in Mining and Underground Constructions. eds. E. Nordlund et al., University of Technology, Luleå, Sweden.

Souley, M., Renaud, V., Al Heib, M., Bouffier, C., Laharie, F., Nyström, A., 2018. Numerical investigation of the development of the excavation damaged zone around a deep polymetallic ore mine. International Journal of Rock Mechanics and Mining Sciences, 106, 165-175.

Wyss, M., Brune, J.N., 1968. Seismic moment, stress, and source dimensions for earthquakes in the California-Nevada region. J. Geophys. Res. 73, 4681-4694.



**COGGUS<sup>2</sup>**

**COMPUTATIONAL &  
GEOENVIRONMENTAL GEOMECHANICS  
FOR UNDERGROUND AND SUBSURFACE  
STRUCTURES**

VISIT OUR WEBSITE  
(coming soon)  
coggus2.univ-lorraine.fr

CONTACT  
coggus-2@univ-lorraine.fr



# Mining Production & Microseismic Activity

## Space-time distribution

